

# Magnetic Resonance Imaging as a Tool for the Study of Mouse Models of Autism

Jacob Ellegood<sup>1\*</sup>, R. Mark Henkelman<sup>1,2</sup> and Jason P. Lerch<sup>1,2</sup>

<sup>1</sup>Mouse Imaging Centre, Hospital for Sick Children, Toronto, Ontario, Canada

<sup>2</sup>Department of Medical Biophysics, University of Toronto, Toronto, Ontario, Canada

## Abstract

Autism is a heterogeneous disorder, in both its behaviour and genetics. This heterogeneity has led to inconsistencies in the neuroanatomical findings in human autistic patients. The benefit of a model system, such as the mouse, is that there could be a decrease in the heterogeneity of the genetics and standardization of the environment could be done, in order to determine a specific anatomical phenotype, which is representative of a specific genotype. Magnetic Resonance Imaging (MRI) has been used quite extensively to examine morphological changes in the mouse brain; however, examining volume and tissue microstructure changes in mouse models of autism with MRI, is just in its infancy. This review will discuss the current research on anatomical phenotyping in mouse models of autism.

## Introduction

In Leo Kanner's 1943 paper he evaluated 11 children with differing signs and symptoms, describing what have come to be referred to, as Autism. The children in that study were quite heterogeneous in both their symptoms, and the severity of those symptoms. Autism, as currently defined, is still quite heterogeneous. The three hallmark characteristics of autism, social deficits, communication deficits, and repetitive restrictive behavior, have large ranges in severity. For example, the communication deficits range from a delay in the development of spoken language to a total lack of any communication (American Psychiatric Association, 2000). Autism is a genetic disorder, with a 90% concordance rate in identical twins and a 15-20% risk of autism in siblings. Similar heterogeneity is seen in the genetics, with well over 200 genes associated with Autism [2]. However, no single gene accounts for more than 1-2% of autistic cases [3].

Using Magnetic Resonance Imaging (MRI), one can detect subtle volume and tissue microstructure changes in the brain, in both humans and the mouse [4]. Meta-analyses of human brain imaging papers have revealed some overlap across studies, yet autism imaging research is plagued by inconsistencies [5-8]. The authors of these analyses highlight age and IQ as an explanation for these inconsistencies, which is certainly a factor, but it is also the genetic, environmental, and behavioural heterogeneity that is driving this variability in imaging. In an animal model, such as the mouse, almost all of that heterogeneity could be eliminated as the genetics and the environment can be tightly controlled.

This review will focus on MRI in mouse models of autism. Specifically, examination of how MRI is used to assess differences in volume and tissue microstructure in the mouse brain would be done. The current literature will be discussed, followed by a brief synopsis of where to go from here.

## The Mouse as a Model System

When the sequencing of the human genome was completed [9,10], researchers started to map the genomes of other mammals. The first mammal examined was the mouse [11]. Knowing the genome of the mouse allows one to gain an understating of how the genotype relates to the phenotype: the anatomical or behavioural characteristic of the mouse. The genes and pathways in the mouse are very similar to the human; in fact, there is a 99.5% probability that a gene from the mouse is also recognized in the human [11]. Economical reasons also make the mouse an excellent model for research as well. For one, the

mouse is quite small in size, limiting housing costs. Secondly, a number of different readily available inbred mouse strains exist, which are, within each strain, genetically identical. Genes can be added, deleted or replaced with relative ease in the mouse, allowing the investigation of the effect of any specific gene. A growing inventory of behavioural tests that show characteristics similar to autism has been reported. Combining all of these factors makes the mouse an easy to use and economical model system, with which the consequences of human disease and behavior could be examined.

## Magnetic Resonance Imaging in the Mouse

Where a brain phenotype is unknown, 3D imaging techniques at the mesoscopic scale (which is a range in between microscopic and macroscopic) can detect very subtle differences, which can lead the researcher to a region of interest, for further examination at the microscopic scale [12].

Examples of mesoscopic 3D imaging techniques [12], used in the mouse are Computed Tomography (CT), which is used frequently for investigating high density structures like bone [4], or vascular trees that have been filled with X-ray opaque contrast agents [13,14]. Recently, there has been a growing interest in embryo imaging with microCT, which relies on the use of contrast agents such as iodine, to enhance soft tissue contrast [15-17]. Ultrasound Biomicroscopy (UBM), commonly used for cardiac imaging [18,19] is also useful for studying embryonic development [20]. Positron Emission Tomography (PET) or Single Photon Emission Computed Tomography (SPECT), requires the use of exogenous contrast agents which can be tagged to any molecule, nanoparticle, or cell. Both, however, are difficult to be scaled down from human to mouse [21], and are often combined with other 3D imaging techniques (MRI or CT), to obtain better spatial resolution combined

**\*Corresponding author:** Jacob Ellegood, Mouse Imaging Centre, Hospital for Sick Children, 25 Orde Street, Toronto, Ontario, M5T 3H7, Canada, **E-mail:** [jacob@phenogenomics.ca](mailto:jacob@phenogenomics.ca)

**Received** August 30, 2012; **Accepted** November 16, 2012; **Published** November 19, 2012

**Citation:** Ellegood J, Henkelman RM, Lerch JP (2012) Magnetic Resonance Imaging as a Tool for the Study of Mouse Models of Autism. *Autism* S1:008. doi:10.4172/2165-7890.S1-008

**Copyright:** © 2012 Ellegood J, et al. This is an open-access article distributed under the terms of the Creative Commons Attribution License, which permits unrestricted use, distribution, and reproduction in any medium, provided the original author and source are credited.

with the molecular specificity of the PET/SPECT at low resolution [22]. Optical Projection Tomography (OPT) Imaging, which is basically fluorescence CT, has recently been used to image fixed samples of the brain or embryo of a mouse at quite high resolution [23]. Lastly, the focus of this review, there is Magnetic Resonance Imaging (MRI), which has been used extensively in the brains of both mouse models [24], and human patients.

MRI uses the nuclear magnetic resonance properties of the water molecule to produce an image of the brain, or other organs of interest. MRI has the best soft-tissue contrast of all the 3D imaging techniques. This contrast comes about because water in different regions of the brain interacts differently with the surrounding environment. With MRI, these differences in the water could be harnessed and the MRI sequences could be manipulated, to get differing tissue contrast dependent on our interests. Figure 1 shows the different types of contrast available with MRI imaging.

MRI is not readily scaled from human to mouse due to the decreased signal as the voxels are scaled down, which is caused by less water being within the voxel as they get smaller. The voxel dimensions need to decrease by 10-15 folds in each dimension (human voxel dimensions-1 mm isotropic, mouse voxel dimensions *in-vivo*-0.125 mm isotropic, fixed brain-0.056 mm isotropic), to achieve comparable images in the mouse as in the human. In order to achieve this increase resolution, several modifications to the MR scanner hardware and imaging protocols are required, including specialized radio-frequency coils, an increase in magnetic field strength, and an increase in the scan duration. The long scan duration causes two additional problems: 1) For *in-vivo* scanning, there is a time limit due to the anesthesia limits for mice, typically ~3 hrs, and 2) for fixed imaging, when there is no physiological limitation; the problem becomes scanner time, especially on a shared system. This could be overcome by scanning more than one mouse at a time in parallel; a technique coined "Multiple Mouse MRI" by the Henkelman group at the Mouse Imaging Centre in Toronto [25-27].

Currently, the major application of mouse MRI is neuroscience, with much of the work focused on genetic models. Examples include Huntington's disease [28-31], Alzheimer's disease [32-34], and other mental health diseases like schizophrenia [35,36], and recently, autism [37-39]. Genetic knockouts are also examined to identify the role of specific genes in development, behaviour and aging. Behaviour links tightly with anatomy, with 90% of gene mutations in mice that show a motor/neurological deficit, featuring an MRI detectable anatomic phenotype [40], and surprisingly even learning and memory can

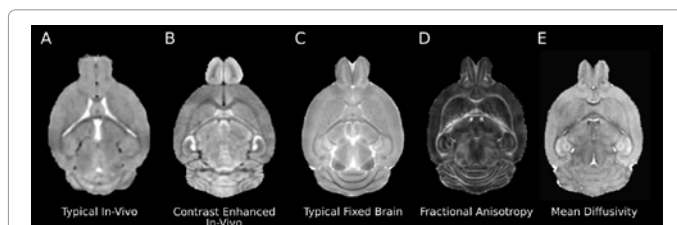


**Figure 1:** Example images highlighting the different tissue contrasts available with MRI.

- A) Typical *in-vivo* imaging (resolution  $125 \times 125 \times 125 \mu\text{m}^3$ ).
- B) *In-vivo* imaging with exogenous Mn contrast enhancement (resolution  $125 \times 125 \times 125 \mu\text{m}^3$ ).
- C) Typical fixed brain imaging (resolution  $56 \times 56 \times 56 \mu\text{m}^3$ ).
- D) Fractional Anisotropy (FA) map from Diffusion Tensor Imaging (DTI) (resolution  $78 \times 78 \times 78 \mu\text{m}^3$ ).
- E) Mean Diffusivity (MD) map from DTI (resolution  $78 \times 78 \times 78 \mu\text{m}^3$ ).

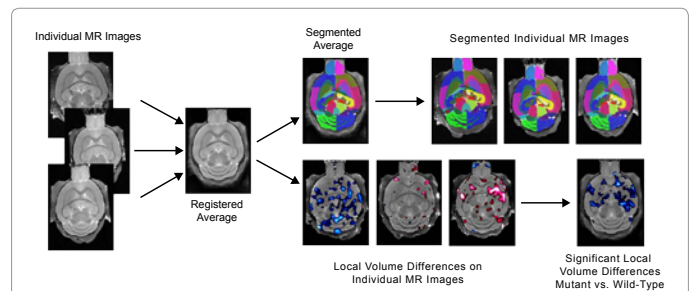


**Figure 2:** The process used for automated analysis. All mice from a particular genetic model, along with their wild-type controls, are scanned with a high resolution post-mortem MRI sequence.

The resulting scans are then automatically aligned towards a common average, segmented with an anatomical atlas, and local volume differences measured.

Final outcomes are anatomical structure volumes per mouse, as well as maps of significant local volume differences (Deformation Based Morphometry).

be detected in neuroanatomical changes. Five days of training in the Morris water maze were sufficient to induce changes in mesoscopic neuroanatomy [41], indicating that anatomical phenotyping could be used to assess learning or other behaviours in the mouse.

## Anatomical Imaging with MRI

Anatomical phenotyping with MRI can be used to examine differences between groups of mice, usually a mutant mouse group versus a control mouse group, with the goal being to determine where in the brain they differ. This could be done by measuring the volumes of brain structures, which gives us a quantitative measure that then can be compared between groups. In some cases, it may be easy to see a difference in volume; for example, the *Engrailed2* Knockout (KO) mouse has a smaller cerebellum, which is clearly visible [42]. However, in other cases, the differences may be quite subtle. Deformation Based Morphometry (DBM) is a commonly used automated technique that can be used to detect anatomical differences between populations. DBM requires no prior hypotheses and produces an unbiased measurement of the volume differences between groups, across the entire brain. DBM is a quantitative image analysis technique which evaluates information contained within the vector field, generated by the nonlinear warping of an individual MRI scan to some sort of reference brain, or to each other [32,43]. DBM has been used previously to examine cross-sectional morphological differences and longitudinal anatomic changes in humans [44], as well as in mouse models [45-47]. Figure 2 is a diagram of the process used for DBM. Using a method such as this, is highly specific and reproducible [48], and with only 10 mice in each group (genetic mutant vs. control), a 5% difference in volume could be detected.

## Diffusion Tensor Imaging (DTI)

DTI is an alternative method used to generate different type of contrast on an MRI image, and can provide quantitative information that can be related to the tissue microstructure. DTI was originally proposed in 1994 by Basser et al. [49], and in that work they estimate, what is called the effective diffusion tensor by measuring the diffusion of water in multiple directions. This diffusion tensor is representative of how water diffuses within a certain voxel, and highlights differences between isotropic (unordered or spherically symmetric) tissues, such as gray matter, and anisotropic (highly ordered) tissues, such as the white matter. The major quantitative measures taken from DTI imaging are Fractional Anisotropy (FA), which measures the degree of anisotropy

(order) in the tissue, and Mean Diffusivity, which is the average diffusion over all directions. A difference in FA is representative of differences in myelination, a change in the tissue permeability, and/or a difference in axonal organization, structure, or size. While differences in FA are not specific to one of these factors (regardless of many researchers attributing a difference in FA to myelination differences), it still reveals a change/difference in the underlying tissue microstructure and highlights an area of interest in the mutant brain.

DTI has become quite useful for examining mouse brain development. Mori et al. [50] at Johns Hopkins University have pioneered the use of diffusion in the mouse brain. Their DTI studies have revealed a characteristic evolution of diffusion anisotropy in the cortex and white matter tracts, throughout the brain during development. This ability to detect changes in the organization of the brain during development can answer questions about both normal and abnormal development. Mori et al. [50] have also looked at different genetic mouse models to examine how the genetics influence the tissue microstructure. One example they looked at was the *Frizzled3* (*Fz3*) KO mouse [51], in which multiple structures and white matter fiber tracts were found to be absent or greatly reduced. Specifically, they found an abnormal U-shaped bundle immediately caudal to the optic tract, which connected the hemispheres of the thalamus; they determined that this tract most likely failed to join the internal capsule at an earlier stage of development. They also examined callosal dysgenesis in two different mouse models, which have a new tract called a Probst bundle [52]. The Probst bundle is an anterior posterior travelling white matter bundle that is caused by a rerouting of the corpus callosum. Thus, DTI provides a wealth of new information about the organization of white matter tracts in the brain, which can help us to better understand the structural connectivity in the brain.

As demonstrated from this previous work in the mouse, using MRI can provide the researcher with an enormous amount of data that identifies previously unknown regions of interest, and may help answer questions about both the effect of genetics or behaviour on the brain.

## Imaging in Autism

In human autism, the results are often compounded by confounds such as age, IQ, environment, genetics, etc. These factors increase the heterogeneity of an already heterogeneous disorder. For example, while some studies report an increase in the size of the hippocampus [53], other studies report a decrease or no change at all [54,55]. Similar differences can be seen with the amygdala [53,55]. In the mouse, the genetics of the subjects could be matched, such that a single genetic mutation could be looked at, and further the environment could be controlled and most of these confounding factors could be eliminated.

## Humans

Several meta-analyses have examined volumetric findings in human autism with MRI, without identifying much consensus. However, there are trends worth mentioning. In 2005, Redclay and Courchesne [56] published a Meta analysis determining when exactly the brain is enlarged in autism, as there have been conflicting reports. They conclude that there is an early period of pathological brain overgrowth, followed by normalization in autism, and this happens during the first 5 years of life. Stanfield et al. [6] performed a meta-analysis on structural MRI studies, in order to determine the neuroanatomy of Autism. They also looked at the total brain and found that it increased in size as well as the cerebral hemispheres, cerebellum, and caudate nucleus, whereas the corpus callosum was reduced. They also noted that the inconsistencies

in the literature might relate to differences in age and IQ, as well as different regions showing abnormal growth trajectories. A review that summarizes the findings from structural MRI studies of human autism has recently been published by Stigler et al. [57].

While these studies highlight some consistent anatomical findings in autism, there is no possibility of accurately diagnosing a child with autism, using structural MRI findings alone. The most consistent, well replicated finding is the reported decrease in size or thinning of the corpus callosum, and there are still reports that have not found differences. Two possible causes lead to this inconsistency: 1) The noise of the given study is too high to find the subtle changes that are happening in the brain, and 2) there are multiple causes of autism (i.e. different genes) that result in different anatomical correlates, yet produce similar behavioural symptoms. Thus, a model system in which the heterogeneity of the genetics could be decreased and the environment could be standardized is needed, which makes the mouse ideal.

## Mouse

As mentioned previously, human autism is defined by three behavioural characteristics: social deficits, communication deficits, and repetitive restrictive behaviours. While it may follow that autism in the mouse should be equivalently behaviourally diagnosed, how to determine a communication or a social deficit in the mouse? Jacqueline Crawley's lab has pioneered behavioural testing in the mouse to help define autistic behaviour [58-60], and in fact there have been a few behaviourally autistic mouse model strains that have been discovered. An example of a mouse that encompasses all 3 of the core behavioural features of Autism, would be the BTBR mouse [61,62].

For the most part, however, autism in the mouse is defined only through genetics. Autism related syndromes account for a small portion of autistic patients. The rest of the autism population is made up of abnormal Copy Number Variations (CNVs), single gene mutations, or currently unknown causes [3]. These unknown cases are thought to be the cause of multiple genetic mutations. Currently, the SFARI gene database lists 200+ genes that have been associated with autism [2], with no single gene accounting for more than 1-2% of autistic cases [3]. Of those 200+ genes, 70+ are listed as having animal models, with that number increasing every year. Typically, the way a new mouse model of autism is created is as follows: a genetic study of a human autistic population is performed, and a genetic mutation is discovered. Then a mouse model, which is representative of that genetic mutation, is created and analyzed to see how it relates to the human case. For example, Jamain et al. [63] found an inherited mutation in the *NeuroLigin3* (*NL3*) gene in a family with two brothers, one with typical autism and the other with Asperger's syndrome. This mutation replaced a highly conserved arginine Residue with Cysteine at amino acid position 451 (R451C), which caused a decrease in the amount of NL3. Tabuchi et al. [64] later introduced that same mutation into a mouse, creating the NL3 R451C Knockin (NL3 KI) mouse model.

Of those 70+ genetic mouse models, less than 10 have published on volumetric analysis using MRI; most of them recently (Table 1). Therefore, using MRI to detect differences in mouse models of autism is just in its infancy. However, there is a growing literature on the subject. Originally, the papers focused on single gene syndromes that were related to autism, such as Fragile X Syndrome (FXS) and Rett Syndrome (RTT). Approximately, 15-33% of the patients with FXS are also classified as having autism, and currently under DSM IV (although this is changing in DSM V), Rett Syndrome is classified as an Autism Spectrum Disorder

Gene/Disorder	Model	Volume Measured	DTI Performed	Paper
Fragile X Syndrome	FMR1 KO	Yes	No	Kooy et al. [65]
	FMR1 KO	Yes	Yes	Ellegood et al. [66]
Rett Syndrome	Mecp2 null	Yes	No	Saywell et al. [67]
	Mecp2 <sup>1lox</sup>	Yes	No	Ward et al. [68]
	Mecp2 <sup>1lox</sup>	Yes	No	Nag et al. [69]
	Mecp2 <sup>308</sup>	Yes	Yes	Ellegood et al.
16p11.2	16p11.2	Yes	No	Horev et al. [70]
Tuberous Sclerosis	Tsc1 +/-	Yes	No	Goorden et al. [71]
Neuroigin3	NL3 KO	Yes	No	Radyushkin et al. [37]
	NL3 KI	Yes	Yes	Ellegood et al. [38]
Integrinβ3	ITGβ3 KO	Yes	No	Ellegood et al. [39]
BALBC/J	Social	No	Yes	Kumar et al. [72]

**Table 1:** Studies that have examined volume and Diffusion Tensor Imaging (DTI) changes with MRI in mouse models related to autism.

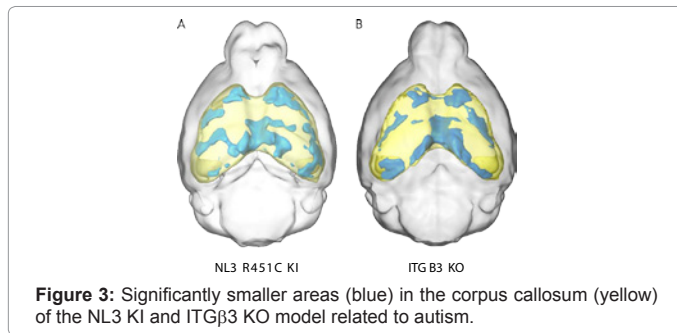
(ASD). One of the first papers to examine with MRI, a mouse model related to autism looked at FXS [65]. FXS is caused when the Fragile X Mental Retardation 1 (FMR1) gene is mutated by a small part of the gene sequence being repeated (the more repeats, the more severe the phenotype). In 1994, the Dutch-Belgian Fragile X Consortium created the first FMR1 mouse, in order to study the physiological role of the FMR1 gene [66]. In 1999, the same group studied the neuroanatomy of the FMR1 mouse using high resolution MRI [65], and although they didn't find any significant difference between groups in that original paper, they hypothesized that "the method described may find wide application in the study of mutant mouse models with neurological involvement". Examination of the FMR1 was revisited in a 2010 study [67]. In contrast to the 1999 FXS study, which examined the volume of 3 regions and the surface area of 7 different regions on a mid-sagittal slice finding no differences, the 2010 study examined 62 different regions in the brain and after accounting for multiple comparisons, 3 regions were highlighted and only one achieved significance, the arbor vita of the cerebellum. The other two regions showed trends towards a decrease in the size of the striatum and an increase in the parieto-temporal lobe. The arbor vita of the cerebellum is composed of both the white matter of the cerebellum and the deep cerebellar nuclei. When the authors investigated this further, they reported that two of the deep cerebellar nuclei were significantly decreased in size, namely the fastigial nucleus and the nucleus interpositus. The authors then proceeded to examine these regions further, using histology and it was concluded that the changes in the nuclei occurred due to a loss of neurons and a subsequent increase in the astrocytes, as a result of reactive gliosis. The anatomical phenotyping performed in such studies is not the end of the investigation. What it does is highlight an area of interest within the brain where a detectable difference is found, which then leads to further investigation.

Several mouse models of Rett Syndrome (RTT) are currently available. They range from full null mutants, who have shortened lifespans of ~8 weeks, to truncation mutations with milder consequences, but similar behavioural characteristics. In 2006, a mouse model of Rett Syndrome, which was a null mutant, was examined with MRI [68]. In this study, volumes were calculated by manual segmentation of the structure on all slices. The authors found an overall reduction in the brain size, a reduction in the thickness of the motor cortex and corpus callosum. Trends were found in the cerebellar volume, as well as noticeable changes in the number of lobules in the cerebellum. This global reduction in overall brain size is a constant feature found in RTT patients. Furthermore, the thinning of the corpus callosum and motor

cortex are also commonly found in RTT. The authors do note, however, that not all the morphologic abnormalities that are found in RTT were seen in the mouse model, as the caudate nucleus and thalamus were not decreased in size in this mouse. In 2008, Ward et al. [69] performed a longitudinal study on the brains of a RTT null mouse from 21 to 42 days of age. They used MRI to calculate 4 different measures of brain development: total brain volume, cerebellar volume, ventricle volume, and motor cortex thickness. Similar to the 2006 study, total brain volume was decreased in the RTT null mice at all time-points in the study, and the cerebellum volume was also decreased initially, but normalized by 42 days of age; however, the motor cortex thinning reported in the 2006 study was not replicated. The same group later assessed the response to environmental enrichment on these same 4 regions [70]. They determined that the environmental enrichment not only improved the performance of the RTT mouse in locomotor and fear conditioning tasks, but it also showed that the ventricular volume negatively correlated with the improved locomotor activity. In 2011, Ellegood et al. [38] examined the brain of the Mecp2<sup>308</sup> truncation RTT mouse (Society for Neuroscience Annual Meeting). They reported the volumes of 62 different structures. Similar to the previous RTT studies, the total brain volume was decreased, and they report volume changes that are consistent with what has been found previously in human RTT. These four studies highlight the power of using MRI to detect volume differences in the brain. Not only are the changes found often replicated in subsequent studies, but also these changes show similar findings to human RTT patients, showing that anatomical phenotyping in mouse models can replicate volumetric abnormalities found in human patients.

Copy number variations are quite common in the human population, and specific CNVs have been found to be associated with autism susceptibility. The long arm of chromosome 16 is an example. A deletion of the 16p11.2 region is associated with autism, while a duplication of this region is associated with both autism and schizophrenia. Recently, Horev et al. [71] created mouse models of 16p11.2 deletion and duplication. These mice were then anatomically phenotyped to look for differences in the brain between groups. In this study, the authors report a strong dosage effect on the volumetric findings in the brain. Specifically, deletions in the 16p11.2 increased brain size, in comparison to controls. Conversely, 16p11.2 duplications lead to decreases. In fact, these mice had dosage dependent effects in gene expression, brain architecture, and behaviour. Furthermore, they found that the deletion was more severe than the duplication. Strong increases in brain size between the 16p11.2 deletion and the WT were found in a number of midline structures, with the hypothalamus findings being the most intriguing. The hypothalamus finding in this study was a previously unreported finding in mouse or human; however, it did account for the behaviour seen in the mouse. Thus, anatomical phenotyping added a previously unknown region of interest that in fact was responsible for the behavioural phenomenon.

Recently, two additional single gene mutations which are associated with autism, have been examined in the mouse. Many common volumetric findings were found in the two models. The two seemingly unrelated models are the Neuroigin3 R451C Knockin (NL3 KI) and the Integrinβ3 Knockout (ITGβ3 KO) mouse. The Neuroigin genes are synaptic adhesion genes located on the postsynaptic membrane, and the ITGβ3 gene's role is to control platelet function, cell adhesion and cell signaling, as well as being related to the serotonin system. Both of these genes have been associated with Autism in separate human studies [63,72]. These mouse models were both studied using the same MRI sequence and analysis [38,39]. The NL3 KI mouse model had marked



volume differences in many different structures, including the total brain volume, which was decreased by 8%. Specific gray matter regions such as the hippocampus, striatum, and thalamus were significantly decreased; in fact, the total gray matter in the brain was decreased by 8%. Similarly, white matter regions had quite strong decreases in size, the corpus callosum, cerebral peduncle, fornix, and internal capsule were all strongly decreased in volume, and the total white matter volume was also decreased by 10%. The ITG $\beta$ 3 KO mouse model also had strong volume differences. Similar to the NL3 KI, the ITG $\beta$ 3 KO mouse's total brain volume was decreased by 11%, and while not all the volume differences were similar to the NL3 KI mouse, there were some striking similarities. 1) In both the NL3 KI and the ITG $\beta$ 3 KO mice, the white matter was strongly affected. White matter differences have become common findings in human autism, with the theory that children undergo a period of abnormal white matter development. Furthermore, white matter deficits in Autism have been thought of as atypical or incomplete connectivity; 2) Volume differences in the corpus callosum have a similar pattern in both models. Figure 3 shows an image of the significant decreases in the corpus callosum in both models. As mentioned, a decreased volume or thinning of the corpus callosum has been one of the most consistent findings in human autism; 3) Both the ITG $\beta$ 3 KO and NL3 KI also had significantly smaller hippocampi, and in both cases, the dentate gyrus and stratum granulosum were much smaller. These similarities between two seemingly unrelated mouse models of Autism highlight a large benefit of the unbiased volumetric measurements performed with Deformation Based Morphometry, using MRI. Anatomical phenotyping can show similarities and differences across the spectrum of autistic models, perhaps grouping some of the genetic causes.

All the white matter volume difference reported in these mouse models, make DTI increasingly necessary to look at the tissue microstructure of the white matter. Only a few studies have looked at mouse models of Autism with DTI. One study examined the FMR1 KO and found no differences in any of the diffusion measures [67]. Another study on the NL3 KI model found only small differences in FA in the globus pallidus of the mouse brain, in spite of the large number of volume differences found in the white matter structures in that model [38]. Given these large volume differences in the white matter in the NL3 KI, the authors were surprised to find a lack of FA differences. They speculated that this could be caused by a loss in the number of axons (a decreased bandwidth), but that the density, size and organization of the axons remained consistent between models. Recently, Kumar et al. [73] used DTI to examine the BALB/CJ mouse. The BALB/CJ mouse is a model of reduced sociability relevant to Autism. In that study, they examined the social behaviour of the BALB/CJ mouse at 3 different time-points and scanned the mice longitudinally with DTI at each of these times. The authors examined 8 manually selected regions of interest (5 gray matter and 3 white matter), in which they reported

trends (as noted in that paper, these findings did not hold up when corrected for multiple comparisons) of higher Mean Diffusivity (MD) in the corpus callosum, and a reduced Fractional Anisotropy (FA) in the external capsule. They attribute the change in FA in the external capsule to reduced myelination, although it could also be attributed to a change in the structure or density of the axons in that region.

## Conclusions and Future Directions

Anatomical phenotyping at the mesoscopic scale in autism is obviously still in its infancy and no strong conclusions about autism, as a whole can be made from the imaging that has been performed so far. In spite of the findings that the ITG $\beta$ 3 KO and NL3 KI have similar anatomical characteristics, there is no great overlap across the small number of mouse models of autism that have been examined currently, and perhaps one should not be expected. The anatomical findings of each individual gene or CNV are certainly relatable to the same genetic case in the human population, as illustrated by the RTT findings. With the 70+ mouse models of autism currently existing and <10 models examined, a larger overlap or grouping of models could not be found, until more are investigated. The goal should be to examine as many models of Autism, in as similar a way as possible. Then the findings from all of those mice should be pooled together to cluster the different models based on their neuroanatomical findings. These clusters could then give rise to different Autism subsets allowing for different treatments. This in turn, could lead to better individual treatments of human autism.

## References

1. Kanner L (1943) Autistic Disturbances of Affective Contact. *Nerv Child* 2: 217-250.
2. Banerjee-Basu S, Packer A (2010) SFARI Gene: an evolving database for the autism research community. *Dis Model Mech* 3: 133-135.
3. Abrahams BS, Geschwind DH (2010) Connecting genes to brain in the autism spectrum disorders. *Arch Neurol* 67: 395-399.
4. Nieman BJ, Flenniken AM, Adamson SL, Henkelman RM, Sled JG (2006) Anatomical phenotyping in the brain and skull of a mutant mouse by magnetic resonance imaging and computed tomography. *Physiol Genomics* 24: 154-162.
5. Frazier TW, Hardan AY (2009) A meta-analysis of the corpus callosum in autism. *Biol Psychiatry* 66: 935-941.
6. Stanfield AC, McIntosh AM, Spencer MD, Philip R, Gaur S, et al. (2008) Towards a neuroanatomy of autism: A systematic review and meta-analysis of structural magnetic resonance imaging studies. *Eur Psychiatry* 23: 289-299.
7. Radua J, Via E, Catani M, Mataix-Cols D (2011) Voxel-based meta-analysis of regional white-matter volume differences in autism spectrum disorder versus healthy controls. *Psychol Med* 41: 1539-1550.
8. Via E, Radua J, Cardoner N, Happé F, Mataix-Cols D (2011) Meta-analysis of gray matter abnormalities in autism spectrum disorder: should Asperger disorder be subsumed under a broader umbrella of autistic spectrum disorder? *Arch Gen Psychiatry* 68: 409-418.
9. Lander ES, Linton LM, Birren B, Nusbaum C, Zody MC, et al. (2001) Initial sequencing and analysis of the human genome. *Nature* 409: 860-921.
10. Venter JC, Adams MD, Myers EW, Li PW, Mural RJ, et al. (2001) The sequence of the human genome. *Science* 291: 1304-1351.
11. Waterston RH, Lindblad-Toh K, Birney E, Rogers J, Abril JF, et al. (2002) Initial sequencing and comparative analysis of the mouse genome. *Nature* 420: 520-562.
12. Henkelman RM (2010) Systems biology through mouse imaging centers: experience and new directions. *Annu Rev Biomed Eng* 12: 143-166.
13. Kampschulte M, Brinkmann A, Stieger P, Sedding DG, Dierkes C, et al. (2010) Quantitative CT imaging of the spatio-temporal distribution patterns of vasa

- vasorum in aortas of apoE-/-/LDL-/- double knockout mice. *Atherosclerosis* 212: 444-450.
14. Yang J, Yu LX, Rennie MY, Sled JG, Henkelman RM (2010) Comparative structural and hemodynamic analysis of vascular trees. *Am J Physiol Heart Circ Physiol* 298: H1249-H1259.
  15. Wong MD, Dorr AE, Walls JR, Lerch JP, Henkelman RM (2012) A novel 3D mouse embryo atlas based on micro-CT. *Development* 139: 3248-3256.
  16. Metscher BD (2009) MicroCT for developmental biology: a versatile tool for high-contrast 3D imaging at histological resolutions. *Dev Dyn* 238: 632-640.
  17. Degenhardt K, Wright AC, Horng D, Padmanabhan A, Epstein JA (2010) Rapid 3D phenotyping of cardiovascular development in mouse embryos by micro-CT with iodine staining. *Circ Cardiovasc Imaging* 3: 314-322.
  18. Phoon CK, Ji RP, Aristizábal O, Worrall DM, Zhou B (2004) Embryonic heart failure in NFATc1-/- mice: novel mechanistic insights from in utero ultrasound biomicroscopy. *Circ Res* 95: 92-99.
  19. Zhou YQ, Foster FS, Nieman BJ, Davidson L, Chen XJ, et al. (2004) Comprehensive transthoracic cardiac imaging in mice using ultrasound biomicroscopy with anatomical confirmation by magnetic resonance imaging. *Physiol Genomics* 18: 232-244.
  20. Turnbull DH, Bloomfield TS, Baldwin HS, Foster FS, Joyner AL (1995) Ultrasound backscatter microscope analysis of early mouse embryonic brain development. *Proc Natl Acad Sci U S A* 92: 2239-2243.
  21. Yang Y, Tai YC, Siegel S, Newport DF, Bai B, et al. (2004) Optimization and performance evaluation of the microPET II scanner for *in vivo* small-animal imaging. *Phys Med Biol* 49: 2527-2545.
  22. Cherry SR (2009) Multimodality imaging: beyond PET/CT and SPECT/CT. *Semin Nucl Med* 39: 348-353.
  23. Sharpe J, Ahlgren U, Perry P, Hill B, Ross A, et al. (2002) Optical projection tomography as a tool for 3D microscopy and gene expression studies. *Science* 296: 541-545.
  24. Nieman BJ, Bock NA, Bishop J, Chen XJ, Sled JG, et al. (2005) Magnetic resonance imaging for detection and analysis of mouse phenotypes. *NMR Biomed* 18: 447-468.
  25. Dazai J, Bock NA, Nieman BJ, Davidson LM, Henkelman RM, et al. (2004) Multiple mouse biological loading and monitoring system for MRI. *Magn Reson Med* 52: 709-715.
  26. Nieman BJ, Bock NA, Bishop J, Sled JG, Josette Chen X, et al. (2005) Fast spin-echo for multiple mouse magnetic resonance phenotyping. *Magn Reson Med* 54: 532-537.
  27. Bock NA, Nieman BJ, Bishop JB, Mark Henkelman R (2005) *In vivo* multiple-mouse MRI at 7 Tesla. *Magn Reson Med* 54: 1311-1316.
  28. Lerch JP, Carroll JB, Dorr A, Spring S, Evans AC, et al. (2008) Cortical thickness measured from MRI in the YAC128 mouse model of Huntington's disease. *Neuroimage* 41: 243-251.
  29. Zhang J, Peng Q, Li Q, Jahanshad N, Hou Z, et al. (2010) Longitudinal characterization of brain atrophy of a Huntington's disease mouse model by automated morphological analyses of magnetic resonance images. *Neuroimage* 49: 2340-2351.
  30. Sawiak SJ, Wood NI, Williams GB, Morton AJ, Carpenter TA (2009) Use of magnetic resonance imaging for anatomical phenotyping of the R6/2 mouse model of Huntington's disease. *Neurobiol Dis* 33: 12-19.
  31. Aggarwal M, Duan W, Hou Z, Rakesh N, Peng Q, et al. (2012) Spatiotemporal mapping of brain atrophy in mouse models of Huntington's disease using longitudinal *in vivo* magnetic resonance imaging. *Neuroimage* 60: 2086-2095.
  32. Lau JC, Lerch JP, Sled JG, Henkelman RM, Evans AC, et al. (2008) Longitudinal neuroanatomical changes determined by deformation-based morphometry in a mouse model of Alzheimer's disease. *Neuroimage* 42: 19-27.
  33. Wadghiri YZ, Hoang DM, Wisniewski T, Sigurdsson EM (2012) *In vivo* magnetic resonance imaging of amyloid- $\beta$  plaques in mice. *Methods Mol Biol* 849: 435-451.
  34. Lerch JP, Pruessner J, Zijdenbos AP, Collins DL, Teipel SJ, et al. (2008) Automated cortical thickness measurements from MRI can accurately separate Alzheimer's patients from normal elderly controls. *Neurobiol Aging* 29: 23-30.
  35. Torres G, Hallas BH, Gross KW, Sperryak JA, Horowitz JM (2008) Magnetic resonance imaging and spectroscopy in a mouse model of schizophrenia. *Brain Res Bull* 75: 556-561.
  36. Poole DS, Oitzl MS, van der Weerd L (2011) MRI in animal models of psychiatric disorders. *Methods Mol Biol* 771: 309-335.
  37. Radyushkin K, Hammerschmidt K, Boretius S, Varoqueaux F, El-Kordi A, et al. (2009) Neuroligin-3-deficient mice: model of a monogenic heritable form of autism with an olfactory deficit. *Genes Brain Behav* 8: 416-425.
  38. Ellegood J, Lerch JP, Henkelman RM (2011) Brain abnormalities in a Neuroligin3 R451C knockin mouse model associated with autism. *Autism Res* 4: 368-376.
  39. Ellegood J, Henkelman RM, Lerch JP (2012) Neuroanatomical Assessment of the Integrin  $\beta 3$  Mouse Model Related to Autism and the Serotonin System Using High Resolution MRI. *Front Psychiatry* 3: 37.
  40. Nieman BJ, Lerch JP, Bock NA, Chen XJ, Sled JG, et al. (2007) Mouse behavioral mutants have neuroimaging abnormalities. *Hum Brain Mapp* 28: 567-575.
  41. Lerch JP, Yiu AP, Martinez-Canabal A, Pekar T, Bohbot VD, et al. (2011) Maze training in mice induces MRI-detectable brain shape changes specific to the type of learning. *Neuroimage* 54: 2086-2095.
  42. Joyner AL, Herrup K, Auerbach BA, Davis CA, Rossant J (1991) Subtle cerebellar phenotype in mice homozygous for a targeted deletion of the En-2 homeobox. *Science* 251: 1239-1243.
  43. Davatzikos C, Vaillant M, Resnick SM, Prince JL, Letovsky S, et al. (1996) A computerized approach for morphological analysis of the corpus callosum. *J Comput Assist Tomogr* 20: 88-97.
  44. Janke AL, de Zubicaray G, Rose SE, Griffin M, Chalk JB, et al. (2001) 4D deformation modeling of cortical disease progression in Alzheimer's dementia. *Magn Reson Med* 46: 661-666.
  45. Zhang J, Chen YB, Hardwick JM, Miller MI, Plachez C, et al. (2005) Magnetic resonance diffusion tensor microimaging reveals a role for Bcl-x in brain development and homeostasis. *J Neurosci* 25: 1881-1888.
  46. Verma R, Mori S, Shen D, Yarowsky P, Zhang J, et al. (2005) Spatiotemporal maturation patterns of murine brain quantified by diffusion tensor MRI and deformation-based morphometry. *Proc Natl Acad Sci U S A* 102: 6978-6983.
  47. Spring S, Lerch JP, Henkelman RM (2007) Sexual dimorphism revealed in the structure of the mouse brain using three-dimensional magnetic resonance imaging. *Neuroimage* 35: 1424-1433.
  48. Kovacević N, Henderson JT, Chan E, Lifshitz N, Bishop J, et al. (2005) A three-dimensional MRI atlas of the mouse brain with estimates of the average and variability. *Cereb Cortex* 15: 639-645.
  49. Basser PJ, Mattiello J, LeBihan D (1994) Estimation of the effective self-diffusion tensor from the NMR spin echo. *J Magn Reson B* 103: 247-254.
  50. Mori S, Itoh R, Zhang J, Kaufmann WE, van Zijl PC, et al. (2001) Diffusion tensor imaging of the developing mouse brain. *Magn Reson Med* 46: 18-23.
  51. Wang Y, Zhang J, Mori S, Nathans J (2006) Axonal growth and guidance defects in Frizzled3 knock-out mice: a comparison of diffusion tensor magnetic resonance imaging, neurofilament staining, and genetically directed cell labeling. *J Neurosci* 26: 355-364.
  52. Ren T, Zhang J, Plachez C, Mori S, Richards LJ (2007) Diffusion tensor magnetic resonance imaging and tract-tracing analysis of Probst bundle structure in Netrin1- and DCC-deficient mice. *J Neurosci* 27: 10345-10349.
  53. Sparks BF, Friedman SD, Shaw DW, Aylward EH, Echelard D, et al. (2002) Brain structural abnormalities in young children with autism spectrum disorder. *Neurology* 59: 184-192.
  54. Haznedar MM, Buchsbaum MS, Wei TC, Hof PR, Cartwright C, et al. (2000) Limbic circuitry in patients with autism spectrum disorders studied with positron emission tomography and magnetic resonance imaging. *Am J Psychiatry* 157: 1994-2001.
  55. Aylward EH, Minshew NJ, Goldstein G, Honeycutt NA, Augustine AM, et al. (1999) MRI volumes of amygdala and hippocampus in non-mentally retarded autistic adolescents and adults. *Neurology* 53: 2145-2150.
  56. Redcay E, Courchesne E (2005) When is the brain enlarged in Autism? A meta-analysis of all brain size reports. *Biol Psychiatry* 58: 1-9.

57. Stigler KA, McDonald BC, Anand A, Saykin AJ, McDougle CJ (2011) Structural and functional magnetic resonance imaging of autism spectrum disorders. *Brain Res* 1380: 146-161.
58. Crawley JN (2004) Designing mouse behavioral tasks relevant to autistic-like behaviors. *Ment Retard Dev Disabil Res Rev* 10: 248-258.
59. Crawley JN (2007) Mouse behavioral assays relevant to the symptoms of autism. *Brain Pathol* 17: 448-459.
60. Moy SS, Nadler JJ, Poe MD, Nonneman RJ, Young NB, et al. (2008) Development of a mouse test for repetitive, restricted behaviors: relevance to autism. *Behav Brain Res* 188: 178-194.
61. McFarlane HG, Kusek GK, Yang M, Phoenix JL, Bolivar VJ, et al. (2008) Autism-like behavioral phenotypes in BTBR T+tf/J mice. *Genes Brain Behav* 7: 152-163.
62. Moy SS, Nadler JJ, Young NB, Perez A, Holloway LP, et al. (2007) Mouse behavioral tasks relevant to autism: phenotypes of 10 inbred strains. *Behav Brain Res* 176: 4-20.
63. Jamain S, Quach H, Betancur C, Råstam M, Colineaux C, et al. (2003) Mutations of the X-linked genes encoding neuroligins NLGN3 and NLGN4 are associated with autism. *Nat Genet* 34: 27-29.
64. Tabuchi K, Blundell J, Etherton MR, Hammer RE, Liu X, et al. (2007) A neuroligin-3 mutation implicated in autism increases inhibitory synaptic transmission in mice. *Science* 318: 71-76.
65. Kooy RF, Reyniers E, Verhoye M, Sijbers J, Bakker CE, et al. (1999) Neuroanatomy of the fragile X knockout mouse brain studied using in vivo high resolution magnetic resonance imaging. *Eur J Hum Genet* 7: 526-532.
66. (1994) Fmr1 knockout mice: a model to study fragile X mental retardation. The Dutch-Belgian Fragile X Consortium. *Cell* 78:23-33.
67. Ellegood J, Pacey LK, Hampson DR, Lerch JP, Henkelman RM (2010) Anatomical phenotyping in a mouse model of fragile X syndrome with magnetic resonance imaging. *Neuroimage* 53: 1023-1029.
68. Saywell V, Viola A, Confort-Gouny S, Le Fur Y, Villard L, et al. (2006) Brain magnetic resonance study of *Mecp2* deletion effects on anatomy and metabolism. *Biochem Biophys Res Commun* 340: 776-783.
69. Ward BC, Agarwal S, Wang K, Berger-Sweeney J, Kolodny NH (2008) Longitudinal brain MRI study in a mouse model of Rett Syndrome and the effects of choline. *Neurobiol Dis* 31: 110-119.
70. Nag N, Moriuchi JM, Peitzman CGK, Ward BC, Kolodny NH, et al. (2009) Environmental enrichment alters locomotor behaviour and ventricular volume in *Mecp2<sup>fllox</sup>* mice. *Behav Brain Res* 196: 44-48.
71. Horev G, Ellegood J, Lerch JP, Son YEE, Muthuswamy L, et al. (2011) Dosage-dependent phenotypes in models of 16p11.2 lesions found in autism. *Proc Natl Acad Sci U S A* 108: 17076-17081.
72. Weiss LA, Kosova G, Delahanty RJ, Jiang L, Cook EH, et al. (2006) Variation in ITGB3 is associated with whole-blood serotonin level and autism susceptibility. *Eur J Hum Genet* 14: 923-931.
73. Kumar M, Kim S, Pickup S, Chen R, Fairless AH, et al. (2012) Longitudinal in-vivo diffusion tensor imaging for assessing brain developmental changes in BALB/cJ mice, a model of reduced sociability relevant to autism. *Brain Res* 1455: 56-67.

This article was originally published in a special issue, [Animal Models in Autism](#) handled by Editor(s), Dr. Craig M. Powell, The University of Texas Southwestern Medical Center Dallas, USA